International Journal of Nanomedicine

Dovepress
open access to scientific and medical research

Open Access Full Text Article

ORIGINAL RESEARCH

Biomimetic piezoelectric nanocomposite membranes synergistically enhance osteogenesis of deproteinized bovine bone grafts

This article was published in the following Dove Press journal:
International Journal of Nanomedicine

Yunyang Bai[1–3]
Xiaohan Dai[4]
Ying Yin[4]
Jiaqi Wang[4]
Xiaowen Sun[3]
Weiwei Liang[1]
Yiping Li[4]
Xuliang Deng[1,5,6]
Xuehui Zhang[3,5,6]

[1]Department of Geriatric Dentistry, Peking University School and Hospital of Stomatology, Beijing 100081, People's Republic of China; [2]Department of Prosthodontics, Peking University School and Hospital of Stomatology, Beijing 100081, People's Republic of China; [3]Department of Dental Materials & Dental Medical Devices Testing Center, Peking University School and Hospital of Stomatology, Beijing 100081, People's Republic of China; [4]Xiangya Stomatological Hospital, Central South University, Changsha 410078, People's Republic of China; [5]National Engineering Laboratory for Digital and Material Technology of Stomatology, Peking University School and Hospital of Stomatology, Beijing 100081, People's Republic of China; [6]Beijing Laboratory of Biomedical Materials, Peking University School and Hospital of Stomatology, Beijing 100081, People's Republic of China

Correspondence: Xuliang Deng
Department of Geriatric Dentistry, Peking University School and Hospital of Stomatology, Zhongguancun South Ave No. 22, Beijing 100081, People's Republic of China
Tel +86 108 219 5637
Fax +86 106 217 3403
Email kqdengxuliang@bjmu.edu.cn

Xuehui Zhang
Department of Dental Materials & Dental Medical Devices Testing Center, Peking University School and Hospital of Stomatology, Zhongguancun South Ave No. 22, Beijing 100081, People's Republic of China
Tel +86 108 219 5748
Fax +86 106 216 4691
Email zhangxuehui@bjmu.edu.cn

Purpose: The combination of a bone graft with a barrier membrane is the classic method for guided bone regeneration (GBR) treatment. However, the insufficient osteoinductivity of currently-available barrier membranes and the consequent limited bone regeneration often inhibit the efficacy of bone repair. In this study, we utilized the piezoelectric properties of biomaterials to enhance the osteoinductivity of barrier membranes.

Methods: A flexible nanocomposite membrane mimicking the piezoelectric properties of natural bone was utilized as the barrier membrane. Its therapeutic efficacy in repairing critical-sized rabbit mandible defects in combination with xenogenic grafts of deproteinized bovine bone (DBB) was explored. The nanocomposite membranes were fabricated with a homogeneous distribution of piezoelectric $BaTiO_3$ nanoparticles (BTO NPs) embedded within a poly(vinylidene fluoridetrifluoroethylene) (P(VDF-TrFE)) matrix.

Results: The piezoelectric coefficient of the polarized nanocomposite membranes was close to that of human bone. The piezoelectric coefficient of the polarized nanocomposite membranes was highly stable, with more than 90% of the original piezoelectric coefficient (d_{33}) remaining up to 28 days after immersion in culture medium. Compared with commercially-available polytetrafluoroethylene (PTFE) membranes, the polarized BTO/P(VDF-TrFE) nanocomposite membranes exhibited higher osteoinductivity (assessed by immunofluorescence staining for runt-related transcription factor 2 (RUNX-2) expression) and induced significantly earlier neovascularization and complete mature bone-structure formation within the rabbit mandible critical-sized defects after implantation with DBB Bio-Oss® granules.

Conclusion: Our findings thus demonstrated that the piezoelectric BTO/P(VDF-TrFE) nanocomposite membranes might be suitable for enhancing the clinical efficacy of GBR.

Keywords: guided bone regeneration, nanocomposite membrane, piezoelectric effect, osteoinduction

Introduction

Guided bone regeneration (GBR) is the major treatment modality for critical-sized bone defects.[1,2] A combination of bone graft with a barrier membrane is the routine approach for GBR treatment.[3] Currently, xenogenic grafts have wide applications in GBR for bone augmentation because of their ready availability and good osteoconductivity.[4–7] Deproteinized bovine bone (DBB), i.e. Bio-Oss ®, is one of the most widely used xenogenic grafts in clinical dentistry.[8–10] The physical structure and chemical properties of DBB are similar to that of natural bone and it has demonstrated positive osteoconductive properties.[8,11] During clinical GBR treatment, a membranous material is usually used as a barrier to

maintain the state of the graft fillings and prevent the ingrowth of fibrous tissue.[12–15] Unfortunately, most currently-utilized barrier membrane materials do not synergistically match the osteoconductivity of the graft implant materials due to a lack of osteoinductive function. Hence, it is imperative to design biomimetic osteoinductive GBR membranes to promote bone formation.

Physiological electrical properties, such as piezoelectricity, play an important role during bone growth and fracture healing.[16–19] Recently, piezoelectric ceramics, including barium titanate ($BaTiO_3$, BTO),[20–23] potassium sodium niobate (KNN),[24] and lithium niobate (LN),[25–27] have been widely used as bone implant materials because of their excellent biocompatibility and osteoinductivity. In our previous study, BTO nanoparticles (NPs) were incorporated into a polymer matrix such as poly-(l-lactic acid) (PLLA)[28] or poly(vinylidene fluoridetrifluoroethylene) (P(VDF-TrFE))[29] to form an electroactive membrane to enhance calvarial defect repair efficacy (without bone grafts), because of the inherent electrical properties of BTO that mimic the physiological electrical properties of natural bone. Therefore, to improve clinical GBR treatment, we hypothesize that the biomimetic piezoelectric BTO/P(VDF-TrFE) nanocomposite membrane can enhance critical-sized bone defect repair efficacy in combination with DBB grafts.

This study therefore aimed to explore the combined therapeutic effectiveness of piezoelectric BTO/P(VDF-TrFE) nanocomposite membranes and xenogenic DBB grafts in repairing critical-sized bone defects in rabbit mandibles. The membranes were fabricated with a homogeneous distribution of piezoelectric BTO NPs embedded in P(VDF-TrFE) matrix. The physicochemical properties of the nanocomposite membranes, including it's morphology, microstructure, and chemical composition were rigorously analyzed, and it's ferroelectric behavior and piezoelectric properties were characterized at room temperature. Additionally, rat bone marrow mesenchymal stem cells (BM-MSCs) were used to evaluate the osteogenic performance of the nanocomposite membranes in vitro, in comparison with commercially-available polytetrafluoroethylene (PTFE) membranes. A rabbit mandible critical-sized defect model was established to evaluate the therapeutic efficacy of the biomimetic piezoelectric nanocomposite membrane in conjunction with xenogenic DBB grafts.

Materials and methods

Fabrication of BTO/P(VDF-TrFE) nanocomposite membranes

The BTO/P(VDF-TrFE) nanocomposite membranes were fabricated utilizing a protocol modified from our previous work.[29] Briefly, BTO NPs (99.9%, average particle size of 100 nm, Alfa Aesar, Ward Hill, MA, USA) were ultrasonically dispersed in 0.01 mol/L of dopamine hydrochloride (99%, Alfa Aesar) aqueous solution, and stirred for 12 h at 60 °C. Then, the dopamine-modified BTO NPs were added to the P(VDF-TrFE) (65/35 mol% VDF/TrFE, Arkema, Colombes, France) co-polymer powders dissolved in N,N -dimethylformamide (DMF) at 5 vol% of the polymer matrix. After ultrasonication and stirring, a stable suspension was formed, which was then cast into membranes with a thickness of approximately 30 μm. For polarization, the membrane samples were treated using a corona discharge under a DC field of 13 kV at room temperature for 30 min.

Characterization of the nanocomposite membranes

The morphologies and internal structures of the nanocomposite membranes were examined by field emission-scanning electron microscopy (FE-SEM, S-4800, HITACHI, Tokyo, Japan) and X-ray diffraction spectroscopy (XRD, Rigaku D/max 2500 VB2t/PC, Tokyo, Japan) respectively. For the ferroelectric property measurements before corona poling, top copper electrodes with a 4-mm diameter were prepared on the nanocomposite membrane by thermal evaporation. The polarization–electric field (P–E) loop was measured using a commercial ferroelectric analyzer (TF1000, aixACCT Systems GmbH, Aachen, Germany) according to our previous study.[29] The piezoelectric property of the nanocomposite membranes after corona poling was measured as the piezoelectric coefficient (d_{33}), using a piezoelectric coefficient meter (ZJ-3AN, IACAS, Beijing, China). For in vitro electrical stability evaluation, the polarized nanocomposite membranes were immersed in serum-free cell culture medium (Cyagen Bioscience Inc., Guangzhou, China) for 28 days, and then rinsed with ddH_2O, prior to measurement of d_{33}.

Cell culture

Rat BM-MSCs (Cyagen Bioscience Inc.) were cultured in Dulbecco's modified Eagle's medium (DMEM) supplemented with 10% (v/v) fetal bovine serum (FBS) and 100 IU/ml penicillin–streptomycin. The medium was changed every 2–3 days. Upon reaching 80–90% confluence, the BM-MSCs were detached using 0.25% (w/v) trypsin/EDTA (Gibco BRL Life Technologies, Carlsbad, CA, USA). The cells from passages 3 to 5 were used in subsequent experiments.

Immunofluorescence staining

To evaluate the effects of the nanocomposite membranes on the osteogenic differentiation of BM-MSCs, expression of the specific osteogenic marker runt-related transcription factor 2 (RUNX-2) was detected by immunofluorescence staining. Briefly, BM-MSCs (5×10^4 cells/well) were seeded onto polarized nanocomposite membranes in 12-well plates and incubated at 37 °C in a humidified atmosphere with 5% CO_2. The commercially-available PTFE membrane (Cytoplast® TXT-200, Osteogenics Biomedical, Inc., USA) was used as the control sample. After 3 days of non-osteogenic induction culture, the samples were rinsed with phosphate-buffered saline (PBS) solution and fixed in 4% (w/v) paraformaldehyde in PBS solution (pH 7.4) for 30 min at room temperature. The cells were then washed with PBS three times before being permeabilized with 0.1% (w/v) Triton X-100 for 10 min and blocked with 3% (w/v) bovine serum albumin (BSA) for 1 h. Subsequently, the cells were incubated overnight at 4 °C with primary antibodies against RUNX-2 primary antibody (ab23981, Abcam Inc. Cambridge, MA, USA, diluted 1:200). After thorough rinsing to remove excess primary antibody, cells were incubated with goat anti-rabbit IgG (ab150077, Abcam Inc., diluted 1:1000) secondary antibody for 1 h at ambient temperature. After rinsing with PBS, the cells were labeled using Phalloidin-Atto 565 (TRITC, Sigma, St. Louis, MO, USA) to stain actin filaments and visualize the cytoskeleton network. Finally, cell nuclei were counterstained with 2-(4-amidinophenyl)-1H-indole -6-carboxamidine (DAPI; Roche) for 10 min and images of the stained samples were observed under a laser scanning confocal microscopy (Zeiss, LSCM 780, Jena, Germany). The mean fluorescence intensities of positive RUNX-2 expression were analyzed using the Image Pro Plus Software (Media Cybernetics, Rockville, MD, USA). The measurement was performed using a minimum sample size of 20 cells in each group.

Animals and surgical procedures

A total of twelve male rabbits (New Zealand White, weighing about 3.0 kg) were used in this study. Rabbits were divided randomly into two groups: (1) The DBB granules and polarized nanocomposite membrane group; and the (2) the DBB granules and PTFE membrane group. Both sides of the mandible were utilized to create bone defects. Circular critical-sized defects, 8-mm in diameter, were made in the mandible body, as described in our previous study.[30] DBB granules (0.25 g) were implanted into the defects and then either the polarized nanocomposite membrane or PTFE membrane was used to cover the defect. Rabbits from each group were sacrificed by lethal intravenous administration of sodium pentobarbital at 4 and 12 weeks post-implantation. All animals were obtained from the Animal Center of Peking University School and Hospital of Stomatology. All experimental protocols pertaining to the use of animals in this study were approved by the Animal Care and Use Committee of Peking University and followed the procedures for Animal Experimental Ethical Inspection of Peking University.

Histological assessment of bone formation and neovascularization

Tissue processing and sectioning were carried out as previously described.[30] Briefly, tissue samples were fixed in 10% (v/v) neutral buffered formalin for 7 days; decalcified and dehydrated according to standard protocols; embedded in paraffin; and sectioned at 5-μm thickness. Hematoxylin and eosin (H&E) staining and Masson's trichrome staining were performed separately on tissue sections, according to the manufacturer's protocols.

Immunohistochemistry for detecting expression of osteocalcin (OCN) and alpha smooth muscle actin (α-SMA) was performed to evaluate the osteogenic and angiogenic differentiation respectively. Briefly, tissue slides were deparaffinized and rehydrated, and then submerged in hydrogen peroxide to quench peroxidase activity. Before exposure to the primary antibodies against OCN (ab13420, CA 1:100, Abcam) or α-SMA (ab7817, CA 1:100, Abcam), slides were incubated with 1% (w/v) BSA to block non-specific binding. After incubation with primary antibodies overnight at 4 °C, horseradish peroxidase (HRP)-conjugated secondary antibodies were applied to the slides for 1 h at room temperature. Finally, a diaminobenzidine (DAB; Beyotime, Jiangsu, China) kit was used to develop the color, followed by counterstaining with hematoxylin. Slides were then observed under a light

microscope (CX21, Olympus, Tokyo, Japan). For quantitative analysis of newly-formed blood vessels, five randomly selected high power fields (HPFs; 400×) from each group were analyzed and the mean number of blood vessels per HPF for each group was then determined.

Statistical analysis

All quantitative data were expressed as mean ± standard error of the mean (SEM). Statistical analyses were performed using the SPSS 19.0 software (IBM Corp., Armonk, NY, USA). Statistical differences were analyzed using Student's *t*-test for independent samples. Values of $*p<0.05$ was considered statistically significant and $**p<0.01$ was considered highly significant.

Results and discussion

Characterization of BTO/P(VDF-TrFE) nanocomposite membranes

The physicochemical properties of the BTO nanocomposite membranes are shown in Figure 1. The membrane surface was smooth and flat (Figure 1A), and the BTO NPs were evenly distributed throughout the polymer matrix (indicated by the yellow arrows). The cross-sectional SEM micrograph further confirmed the uniform

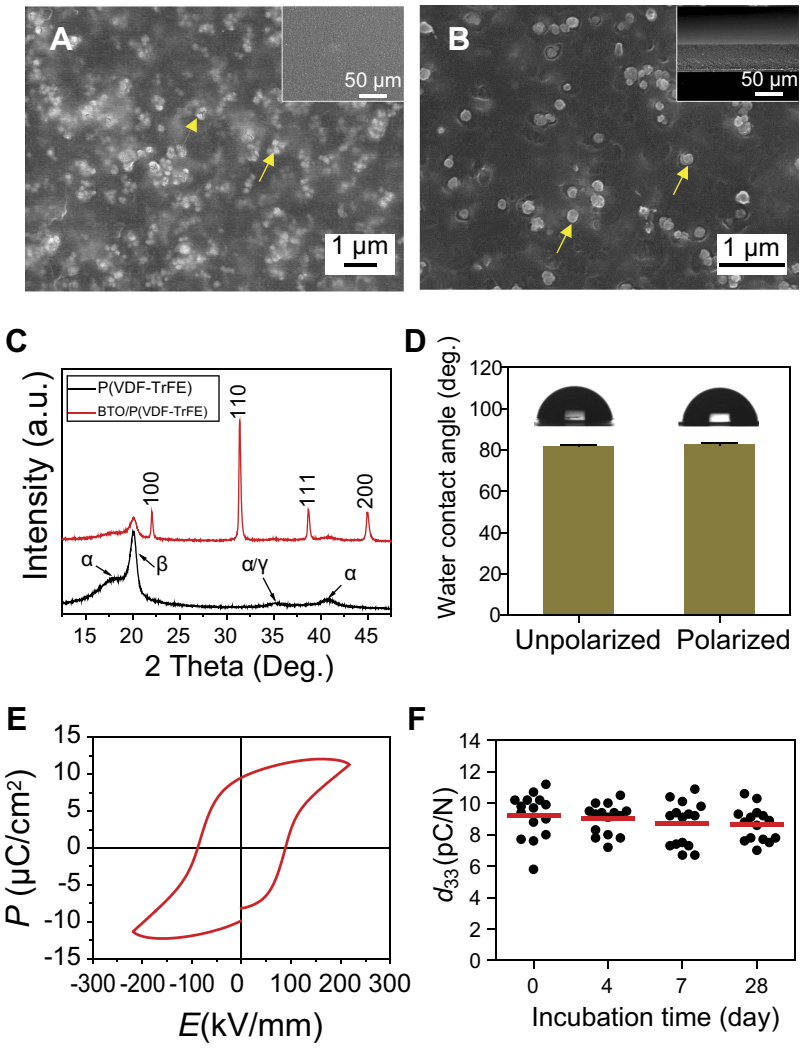

Figure 1 Characterizations of BTO/P(VDF-TrFE) nanocomposite membranes. (**A**) Representative SEM image of the surface morphology of polarized nanocomposite membranes. (**B**) Cross-sectional SEM images of polarized composite membranes. Insets are the low magnification images. Yellow arrows denote the BTO nanoparticles. (**C**) X-Ray diffraction patterns of BTO/P(VDF-TrFE) nanocomposite membranes and neat P(VDF-TrFE) membranes. (**D**) Water contact angles of nanocomposite membrane before and after corona poling treatment. (**E**) The hysteresis loops of nanocomposite membranes. (**F**) The piezoelectric coefficient (d_{33}) values of the polarized nanocomposite membranes after immersion in serum-free cell culture medium for different time durations.

Abbreviations: BTO, $BaTiO_3$; P(VDF-TrFE), poly(vinylidene fluoridetrifluoroethylene); SEM, scanning electron microscopy.

distribution of the BTO NPs within the polymer matrix (Figure 1B). The uniform distribution of the BTO NPs within the polymer matrix is mainly due to surface modification of the BTO NPs with polydopamine. This principle is explained in our previous study,[29] in which a better interface compatibility between the BTO NPs fillers and the P(VDF-TrFE) matrix was achieved by introducing polydopamine surface layers on the BTO NPs, resulting in homogeneous dispersion of BTO particles on the membranes. In the present study, the thickness of the nanocomposite membrane was reduced from ~60 μm in our previous study[29] to approximately 30 μm, making it significantly more flexible, easier to handle clinically, and more conformable to bone defect sites. The XRD patterns exhibited typical BTO crystallization characteristics and the ferroelectric β-phase of the P(VDF-TrFE) was detected (Figure 1C), which indicated that the crystalline characteristics of the piezoelectric ceramic BTO and the ferroelectric phase of the polymer P(VDF-TrFE) remained undisturbed during the fabrication process of the nanocomposite membrane. The β-phase in P(VDF-TrFE) has an important role in the piezoelectric and ferroelectric properties of the material[31] and exert a positive effect on its biological functions.[32]

The water contact angle of the piezoelectric BTO/P(VDF-TrFE) nanocomposite membrane was below 100° but above 80° and this was not significantly altered by the corona poling treatment (Figure 1D), which is similar to that reported in our previous study.[29] The relatively low surface wettability would be advantageous in ensuring the non-stickiness of the implanted membrane to the newly-regenerated bone tissue. This will facilitate easier removal of the membrane after bone defect healing, and also enable sustainable maintenance of the local electric microenvironment, thereby avoiding inflammation and other side effects of residual materials, as demonstrated by our previous research.[29]

The electrical properties of the nanocomposite membranes were then investigated. Typical hysteresis loops were observed in the P-E curves (Figure 1E), which indicated the ferroelectric behavior of the nanocomposite membranes. Interestingly, the maximal polarization (P_m) and residual polarization (P_r) values were 12.06 μC/cm^2 and 9.43 μC/cm^2, respectively, which were higher than that detected in our previous report[28] (6.72 μC/cm^2 and 5.17 μC/cm^2, respectively). This was probably because making the nanocomposite membrane thinner decreased the internal defects within the membrane under the same preparation process conditions, resulting in a high breakdown strength during P-E loop examination.[33,34] The high breakdown strength is beneficial to enhanced electrical polarization, which in turn improved the electrical stability of the composite membrane. Given the importance of the piezoelectric effect on bone regeneration, we further analyzed the piezoelectric properties of the nanocomposite membrane, using the piezoelectric coefficient (d_{33}) as a measure. The results showed that the piezoelectric coefficient of the polarized nanocomposite membranes was about 9.21 pC/N (Figure 1F), which is similar to that of human bone.[35] This thus indicated that the polarized nanocomposite membranes might have the capacity to provide a piezoelectric-mimetic microenvironment that is conducive for cell function and tissue repair.

The electrical stability of the piezoelectric nanocomposite membrane was further evaluated by measuring the d_{33} coefficients for different incubation periods under cell culture conditions. Figure 1F shows that the d_{33} coefficient of the polarized nanocomposite membranes remained stable at more than 90% of its original value for up to 28 days. The remarkable stability of the piezoelectric property of the nanocomposite membrane could be attributed to the high residual polarization, as shown in Figure 1E. The high remnant polarization allows the nanocomposite membrane to stably retain its piezoelectric coefficient, as have been reported previously by other studies[36,37] and our previous work.[29] This outstanding physiological and electrical stability of the BTO/P(VDF-TrFE) membranes could enable them to maintain the local electric microenvironment in situ after implantation, and may exert a positive synergistic effect in guiding bone regeneration during bone filling repair.

In vitro osteogenic differentiation of BM-MSCs on the polarized BTO/P(VDF-TrFE) nanocomposite membranes

Before evaluating the GBR efficacy of the polarized nanocomposite membrane versus the commercially-available PTFE membrane in vivo with the critical-sized rabbit mandibular defect model, we first compared the effects of these two types of barrier membranes on the osteogenic differentiation of BM-MSCs in vitro. RUNX-2 was selected as a marker of osteogenic differentiation because it is an upstream osteogenic differentiation-specific transcription factor that has been widely used in previous studies to

evaluate the osteonductive capacities of biomaterials. The immunofluorescence analysis showed that both types of membranes promoted the adhesion and spreading of BM-MSCs. However, RUNX-2 was weakly expressed by BM-MSCs on the PTFE membrane, but was markedly enhanced on the polarized nanocomposite membrane, being mainly concentrated in the cell nucleus (Figure 2A). This significant difference was also confirmed by the quantitative analysis (Figure 2B), which indicated that the surface of the polarized nanocomposite membrane had a positive osteoinductive effect on BM-MSCs. Our results were consistent with that of previous studies, in which polarized BTO/P(VDF-TrFE) nanocomposite membranes enhanced the expression of bone markers in human alveolar bone-derived cells, as compared to PTFE membranes.[38,39] This osteoinductive effect may be mainly attributed to the polarization charge derived from the composite membrane surface. The persistent polarization charge generated by the residual polarization of ferroelectric biomaterials could positively promote osteoblast activity, as reported by our previous study[28] and other reports.[26,27,32,40] These results implied that the polarized BTO/P(VDF-TrFE) nanocomposite membranes had higher osteoinductivity than the PTFE membrane, which might represent a better material for enhancing bone regeneration.

The effects of barrier membranes on critical-sized mandible bone defect repair

The effects of the polarized BTO/P(VDF-TrFE) nanocomposite membrane on bone graft implantation repair was further investigated by establishing a critical-sized rabbit mandibular bone defect model (Figure 3). The defect area was filled with DBB granules and then covered with either a BTO/P(VDF-TrFE) nanocomposite membrane or a PTFE membrane. As shown in Figure 4, at 4 weeks post-surgery, in both the BTO/P(VDF-TrFE) nanocomposite membrane group and the PTFE membrane group, DBB granules were in close physical contact with the new fibrous connective tissue and there was no obvious inflammatory reaction. Moreover, in the polarized composite membrane group, the nascent tissue grew into the holes of the DBB granule. This thus indicated the good tissue biocompatibility of the DBB. Under high magnification, new bone formation was observed around the DBB granules and a bone marrow-like structure could

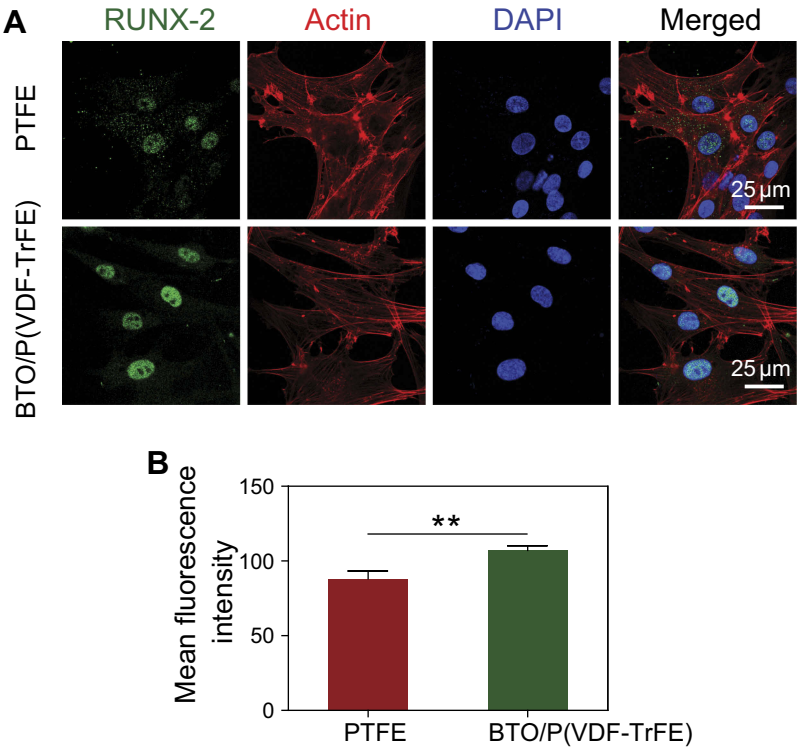

Figure 2 Osteogenic differentiation of BM-MSCs on polarized nanocomposite membranes and commercially-available PTFE membranes. (**A**) Representative immunostaining images for detection of RUNX-2 (green), actin network (red), and cell nuclei (DAPI, blue) in BM-MSCs cultured for 3 days. (**B**) Quantification of the immunostaining intensity of RUNX-2. Error bars represent one standard error. (**$p<0.01$).

Abbreviations: BM-MSCs, bone marrow mesenchymal stem cells; PTFE, polytetrafluoroethylene; RUNX-2, runt-related transcription factor 2; DAPI, 2-(4-amidinophenyl)-1H-indole-6-carboxamidine.

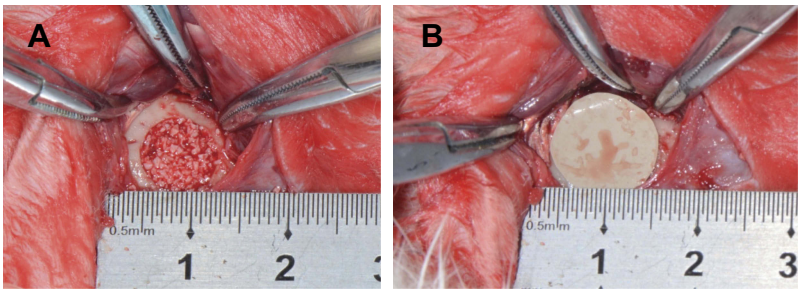

Figure 3 Illustration of the surgical procedure. (**A**) Bone defects with a diameter of 8-mm were created on rabbit mandibles, and then filled with DBB granules. (**B**) Bone defects were covered with polarized BTO/P(VDF-TrFE) nanocomposite membranes or commercially-available PTFE membranes.
Abbreviations: DBB, deproteinized bovine bone; BTO, $BaTiO_3$; P(VDF-TrFE), poly(vinylidene fluoridetrifluoroethylene); PTFE, polytetrafluoroethylene.

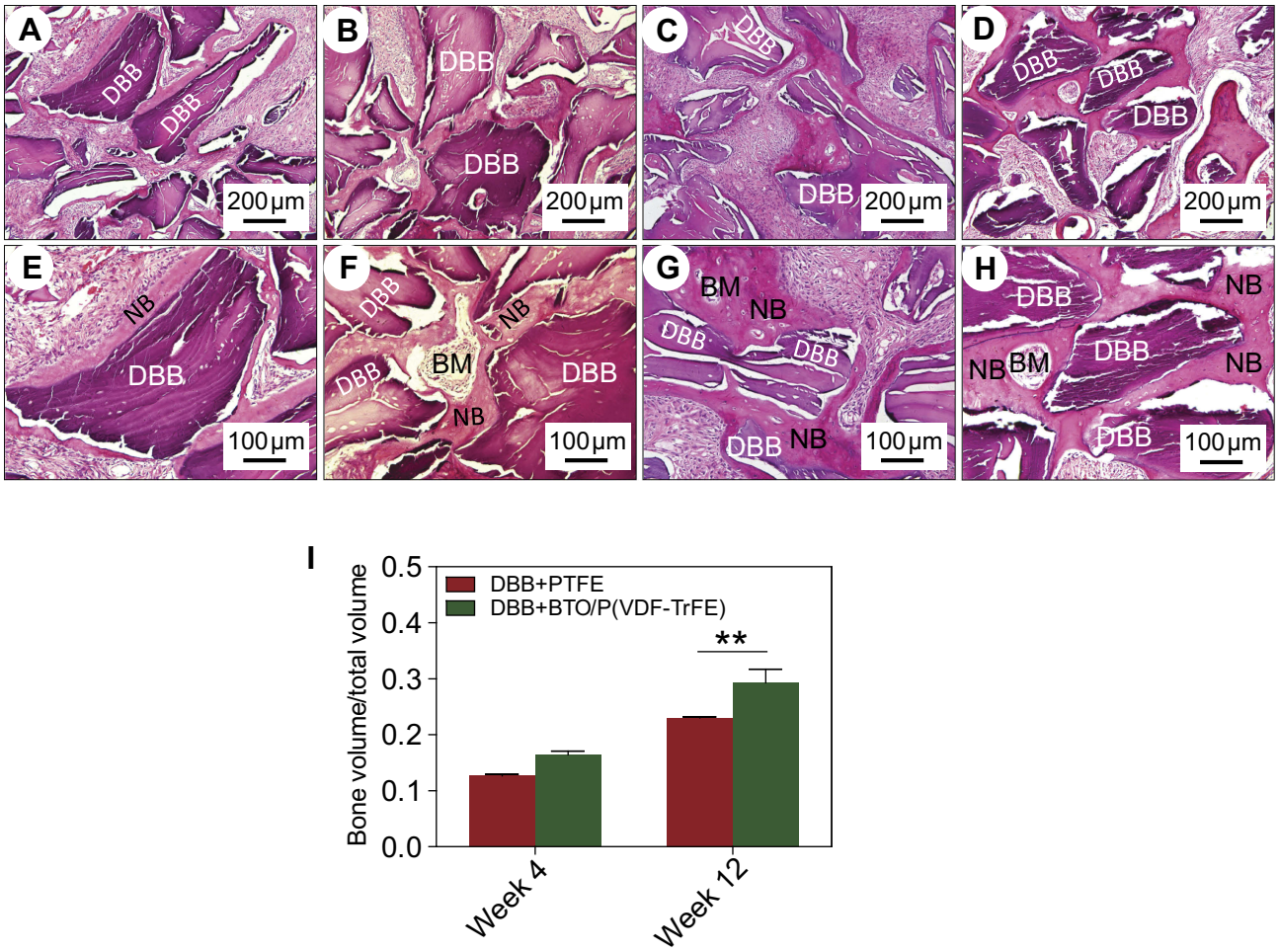

Figure 4 Histological evaluation of bone defects after implantation for 4 weeks and 12 weeks. (**A, B, E, F**) H&E staining images after 4 weeks of implantation. (**A, E**) PTFE membrane group. (**B, F**) BTO/P(VDF-TrFE) membrane group. (**C, D, G, H**) H&E staining images after 12 weeks of implantation. (**C, G**) PTFE membrane group. (**D, H**) BTO/P(VDF-TrFE) membrane group. The lower images are enlargements of specific regions of the upper images. (DBB: deproteinized bovine bone; NB: nascent bone; BM: bone marrow-like tissue). Scale bars =200 μm for (**A**–**D**); Scale bars =100 μm for (**E-H**). (**I**) Quantitative histomorphometry analysis of bone volume/total volume (BV/TV). Error bars represent one standard error. (**$p<0.01$).
Abbreviations: H&E, hematoxylin and eosin; PTFE, polytetrafluoroethylene; BTO, $BaTiO_3$; P(VDF-TrFE), poly(vinylidene fluoridetrifluoroethylene); DBB, deproteinized bovine bone; NB, nascent bone; BM, bone marrow-like tissue.

be seen in the polarized composite membrane group. The quantitative analysis showed that the regenerated bone volume in the polarized composite membrane group was slightly higher than that in the PTFE group. At 12 weeks post-surgery, the H&E staining results showed significant nascent bone formation, with a dense bone structure and

a bone marrow-like structure surrounding the residual DBB granules, in the polarized composite membrane group, whereas less nascent bone tissue formation with a loose bone structure was observed in the PTFE group. This was confirmed by the quantitative analysis, which showed that the BTO/P(VDF-TrFE) nanocomposite membranes yielded a higher bone volume/tissue volume (BV/TV) ratio compared with that of the PTFE membranes ($p<0.01$) (Figure 4I).

To further assess the degree of nascent bone remodeling, new bone formation at 12 weeks post-implantation was characterized using Masson's trichrome staining. In the polarized BTO/P(VDF-TrFE) nanocomposite membrane group, red-stained, dense osteoid bone tissues with active osteocytes (yellow arrows) was observed around the DBB granules (Figure 5A). By contrast, in the PTFE membrane group, new bone tissue with blue-stained mineralized bone was observed (Figure 5B). These results indicated that the polarized nanocomposite membrane markedly enhanced the implantation repair efficacy of DBB grafts and significantly promoted the remodeling and maturity of bone regeneration.

We hypothesized that polarized nanocomposite membranes would exert a positive effect on early neovascularization. As expected, copious nascent blood vessel formation surrounding the DBB granules was observed in the polarized nanocomposite membrane group (Figure 6B), while only a small number of nascent blood vessels were observed in the PTFE membrane group at 4 weeks post-implantation (Figure 6A). The immunohistochemistry results showed a similar trend. Blood vessels were easily identified in the tissue samples (black arrowheads in Figure 6C and D) via positive immunoreactivity with antibodies against α-SMA, a marker of vascular smooth muscle cells.

Quantitative analysis suggested that the number of blood vessels in the polarized nanocomposite membrane group was higher than that in the PTFE membrane group (Figure 6E). These results confirmed the key role of the polarized nanocomposite membranes in promoting early neovascularization. This may be attributed to the surface charge of the polarized nanocomposite membranes, which could stimulate vascular endothelial cell differentiation and promote neovascularization in vivo, as reported previously.[41] Our results were also consistent with other studies, which showed that exogenous electrical stimulation,[41,42] an external electric field,[43,44] or even charged scaffold material,[45] could induce vascular endothelial cell luminal formation in vitro and neovascularization in vivo. Early neovascularization had a profound effect on subsequent bone remodeling and bone maturation. Figure 7 shows that the expression of osteocalcin in the newly-regenerated bone of the polarized nanocomposite membrane group was significantly enhanced. Because Human bone is a highly-vascularized tissue, therefore the development of blood vessel networks within the implanted bone graft materials is of utmost importance. These results thus indicated that polarized nanocomposite membranes and DBB granules had a synergistic effect in promoting bone defect repair by means of active early neovascularization, as shown in Figure 8.

Conclusion

In this study, flexible BTO/P(VDF-TrFE) piezoelectric nanocomposite membranes were fabricated and used as a barrier membrane in guided bone regeneration therapy. The piezoelectric coefficient of the polarized nanocomposite membranes was about 9.21 pC/N, which was close to that of human bone. Compared with commercially-available polytetrafluoroethylene (PTFE) membranes, the polarized nanocomposite membranes exhibited higher osteoinductivity in vitro and induced more copious neovascularization in rabbit

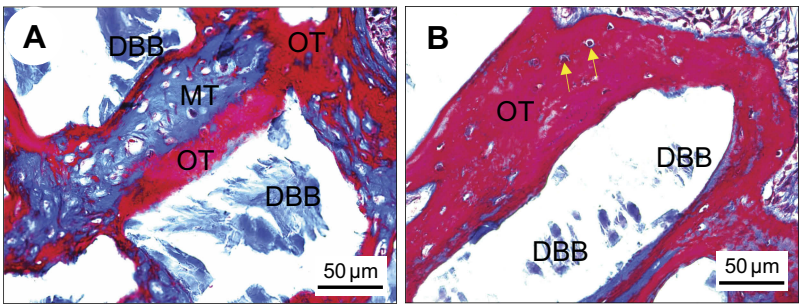

Figure 5 Histological observation of bone restoration after 12 weeks post-implantation. Representative Masson's trichrome staining images of DBB granules within defects covered with PTFE membranes (**A**) or BTO/P(VDF-TrFE) nanocomposite membranes (**B**). Yellow arrows denote viable osteocytes in their lacunae. Scale bar =50 μm.
Abbreviations: DBB, deproteinized bovine bone; OT, osteoid tissue (red); MT, mineralized tissue (blue); PTFE, polytetrafluoroethylene; BTO, $BaTiO_3$; P(VDF-TrFE), poly (vinylidene fluoridetrifluoroethylene).

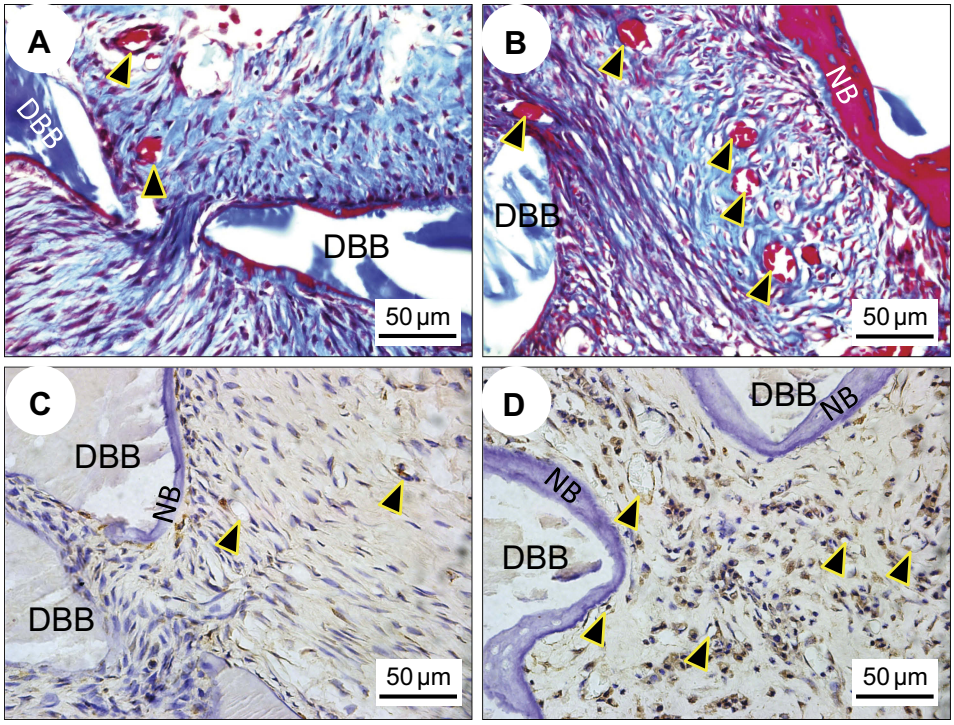

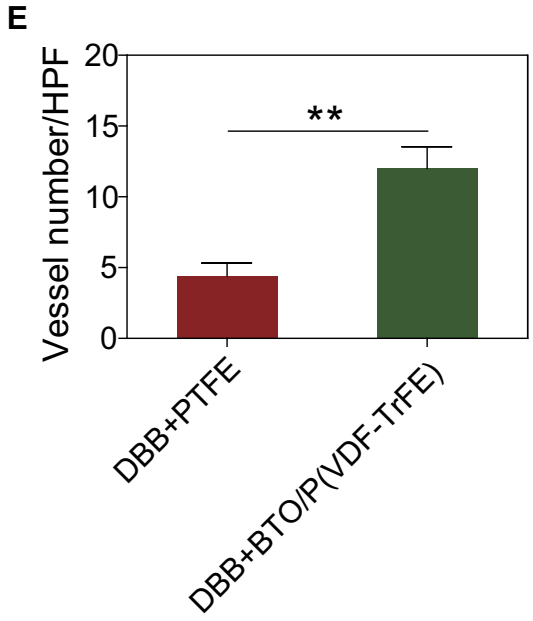

Figure 6 Evaluation of neovascularization at 4 weeks post-implantation. (**A**–**B**) Representative Masson's trichrome staining images after implantation with DBB granules and covering with PTFE membranes (**A**) or BTO/P(VDF-TrFE) nanocomposite membranes (**B**). (**C**–**D**) Immunohistological staining images for detection of α-SMA expression after implantation with DBB granules and covering with PTFE membranes (**C**) or BTO/P(VDF-TrFE) nanocomposite membranes (**D**). (**E**) Quantitative analysis of the number of nascent blood vessels after 4 weeks post-implantation (**$p<0.01$). Black arrowheads denote the nascent blood vessels. Scale bar =50 μm.

Abbreviations: DBB, deproteinized bovine bone; NB, nascent bone; PTFE, polytetrafluoroethylene; BTO, $BaTiO_3$; P(VDF-TrFE), poly(vinylidene fluoridetrifluoroethylene); α-SMA, alpha smooth muscle actin; HPF, high power fields.

mandible critical-sized defects after implantation with Bio-Oss® granules, giving rise to markedly enhanced bone regeneration and complete mature bone-structure formation. These results thus indicated that the designed osteoinductive barrier membranes could improve the outcome of guided bone regeneration. This might provide an innovative and effective strategy for guided bone regeneration therapies.

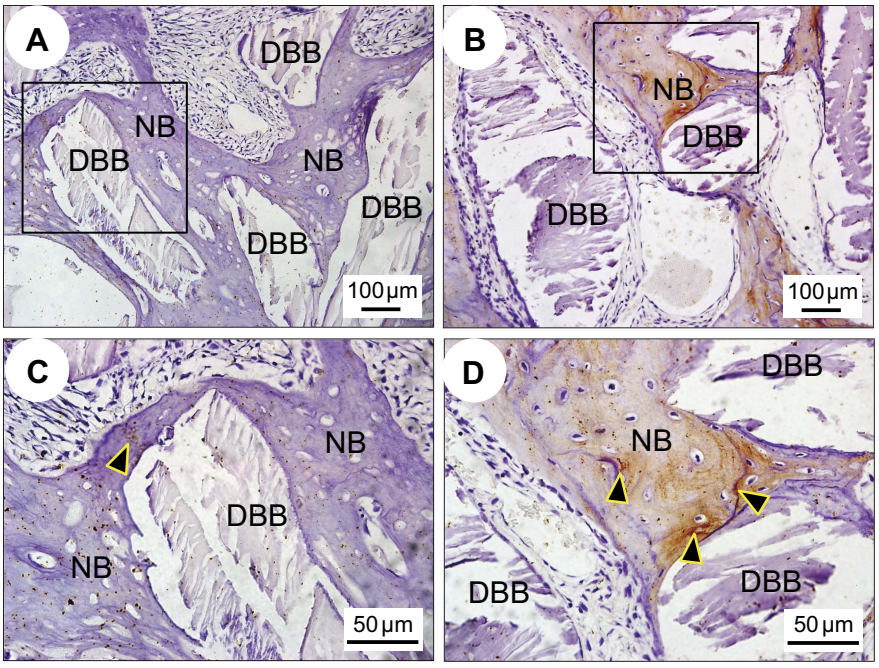

Figure 7 Immunohistochemical evaluation of bone regeneration at 12 weeks post-implantation. Representative immunohistochemical staining images for detection of OCN expression in DBB granules around nascent bone tissues covered with PTFE membranes (**A**) or BTO/P(VDF-TrFE) nanocomposite membranes (**B**). (**C**) and (**D**) are enlargements of specific regions of (**A**) and (**B**) respectively. Black arrowheads denote the positive expression of OCN. Scale bars =100 μm for (**A**–**B**); Scale bars =50 μm for (**C**-**D**).
Abbreviations: OCN, osteocalcin; DBB, deproteinized bovine bone; NB, nascent bone; PTFE, polytetrafluoroethylene; BTO, $BaTiO_3$; P(VDF-TrFE), poly(vinylidene fluoridetrifluoroethylene).

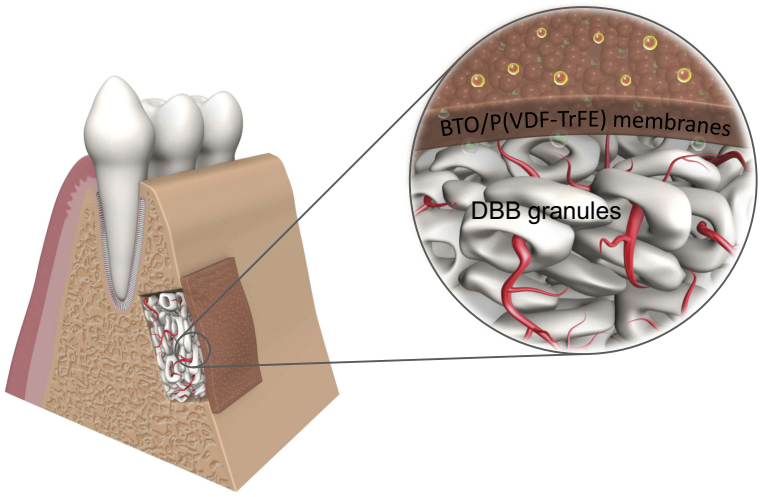

Figure 8 Illustration of the synergistic effects of combining piezoelectric BTO/P(VDF-TrFE) nanocomposite membranes with xenogenic DBB grafts on the repair of critical-sized bone defects. Electric dipoles of BTO NPs are reoriented in the direction of the poling electric field after corona poling treatment, and consequently polarized charges are generated on the surface of BTO/P(VDF-TrFE) nanocomposite membranes. When the membranes are implanted as a barrier membrane covering the bone defect filled with DBB grafts, the electric microenvironment is sustainably maintained, resulting in enhanced neovascularization and rapid bone regeneration, which consequently led to complete mature bone-structure formation integrated with the implanted DBB grafts.
Abbreviations: DBB, deproteinized bovine bone; BTO, $BaTiO_3$; P(VDF-TrFE), poly(vinylidene fluoridetrifluoroethylene).

Acknowledgments

This work was supported by the National Key R&D Program of China (2018YFC1105303, 2018YFC1105304, 2017YFC1104302/03), National Natural Science Foundation of China (Nos. 51772006, 81425007, 31670993, 51502006), Beijing Municipal Science &

Technology Commission Projects (Nos. Z1811000-02018001, Z171100002017009), and the Young Elite Scientist Sponsorship Program by CAST (2016QNRC001).

Disclosure

The authors report no conflicts of interest in this work.

References

1. Stavropoulos F, Nale JC, Ruskin JD. Guided bone regeneration. *Oral Maxillofac Surg Clin North Am*. 2002;14(1):15–27.
2. Wang HL. Principles in guided bone regeneration. *Dent Implantol Update*. 1998;9(5):33–37.
3. Bottino MC, Thomas V, Schmidt G, et al. Recent advances in the development of GTR/GBR membranes for periodontal regeneration–a materials perspective. *Dent Mater*. 2012;28(7):703–721. doi:10.1016/j.dental.2012.04.022
4. Benic GI, Thoma DS, Munoz F, Sanz Martin I, Jung RE, Hammerle CH. Guided bone regeneration of peri-implant defects with particulated and block xenogenic bone substitutes. *Clin Oral Implants Res*. 2016;27(5):567–576. doi:10.1111/clr.12625
5. Elgali I, Turri A, Xia W, et al. Guided bone regeneration using resorbable membrane and different bone substitutes: early histological and molecular events. *Acta Biomater*. 2016;29:409–423. doi:10.1016/j.actbio.2015.10.005
6. Santos Kotake BG, Gonzaga MG, Coutinho-Netto J, Ervolino E, de Figueiredo FAT, Issa JPM. Bone repair of critical-sized defects in Wistar rats treated with autogenic, allogenic or xenogenic bone grafts alone or in combination with natural latex fraction F1. *Biomed Mater*. 2018;13(2):025022. doi:10.1088/1748-605X/aa9504
7. Issa JP, Gonzaga M, Kotake BG, de Lucia C, Ervolino E, Iyomasa M. Bone repair of critical size defects treated with autogenic, allogenic, or xenogenic bone grafts alone or in combination with rhBMP-2. *Clin Oral Implants Res*. 2016;27(5):558–566. doi:10.1111/clr.12622
8. Baldini N, De Sanctis M, Ferrari M. Deproteinized bovine bone in periodontal and implant surgery. *Dent Mater*. 2011;27(1):61–70. doi:10.1016/j.dental.2010.10.017
9. Liu T, Wu G, Wismeijer D, Gu Z, Liu Y. Deproteinized bovine bone functionalized with the slow delivery of BMP-2 for the repair of critical-sized bone defects in sheep. *Bone*. 2013;56(1):110–118. doi:10.1016/j.bone.2013.05.017
10. Wu G, Hunziker EB, Zheng Y, Wismeijer D, Liu Y. Functionalization of deproteinized bovine bone with a coating-incorporated depot of BMP-2 renders the material efficiently osteoinductive and suppresses foreign-body reactivity. *Bone*. 2011;49(6):1323–1330. doi:10.1016/j.bone.2011.09.046
11. Accorsi-Mendonca T, Conz MB, Barros TC, de Sena LA, Soares Gde A, Granjeiro JM. Physicochemical characterization of two deproteinized bovine xenografts. *Braz Oral Res*. 2008;22(1):5–10.
12. Zhang J, Ma S, Liu Z, et al. Guided bone regeneration with asymmetric collagen-chitosan membranes containing aspirin-loaded chitosan nanoparticles. *Int J Nanomedicine*. 2017;12:8855–8866. doi:10.2147/IJN.S148179
13. Wessing B, Lettner S, Zechner W. Guided bone regeneration with collagen membranes and particulate graft materials: a systematic review and meta-analysis. *Int J Oral Maxillofac Implants*. 2018;33(1):87–100. doi:10.11607/jomi.5461
14. Chu C, Deng J, Sun X, Qu Y, Man Y. Collagen membrane and immune response in guided bone regeneration: recent progress and perspectives. *Tissue Eng Part B Rev*. 2017;23(5):421–435. doi:10.1089/ten.TEB.2016.0463
15. Jardini MA, Tera TM, Meyer AA, Moretto CM, Prado RF, Santamaria MP. Guided bone regeneration with or without a collagen membrane in rats with induced diabetes mellitus: histomorphometric and immunolocalization analysis of angiogenesis and bone turnover markers. *Int J Oral Maxillofac Implants*. 2016;31(4):918–927. doi:10.11607/jomi.4358
16. Shamos MH, Lavine LS, Shamos MI. Piezoelectric effect in bone. *Nature*. 1963;197:81. doi:10.1038/197081a0
17. Marino A, Becker RO. Piezoelectric effect and growth control in bone. *Nature*. 1970;228(5270):473–474.
18. Rajabi AH, Jaffe M, Arinzeh TL. Piezoelectric materials for tissue regeneration: a review. *Acta Biomater*. 2015;24:12–23. doi:10.1016/j.actbio.2015.07.010
19. Biranche Tandon JJB, Cartmell SH. Piezoelectric materials as stimulatory biomedical materials and scaffolds for bone repair. *Acta Biomater*. 2018;73:1–20. doi:10.1016/j.actbio.2018.04.026
20. Ehterami A, Kazemi M, Nazari B, Saraeian P, Azami M. Fabrication and characterization of highly porous barium titanate based scaffold coated by Gel/HA nanocomposite with high piezoelectric coefficient for bone tissue engineering applications. *J Mech Behav Biomed Mater*. 2018;79:195–202. doi:10.1016/j.jmbbm.2017.12.034
21. Shokrollahi H, Salimi F, Doostmohammadi A. The fabrication and characterization of barium titanate/akermanite nano-bio-ceramic with a suitable piezoelectric coefficient for bone defect recovery. *J Mech Behav Biomed Mater*. 2017;74:365–370. doi:10.1016/j.jmbbm.2017.06.024
22. Scalize PH, Bombonato-Prado KF, de Sousa LG, et al. Poly(vinylidene fluoride-trifluorethylene)/barium titanate membrane promotes de novo bone formation and may modulate gene expression in osteoporotic rat model. *J Mater Sci Mater Med*. 2016;27(12):180. doi:10.1007/s10856-016-5799-x
23. Teixeira LN, Crippa GE, Trabuco AC, et al. In vitro biocompatibility of poly(vinylidene fluoride–trifluoroethylene)/barium titanate composite using cultures of human periodontal ligament fibroblasts and keratinocytes. *Acta Biomater*. 2010;6:979–989. doi:10.1016/j.actbio.2009.08.024
24. Yu P, Ning C, Zhang Y, et al. Bone-inspired spatially specific piezoelectricity induces bone regeneration. *Theranostics*. 2017;7(13):3387–3397. doi:10.7150/thno.19748
25. Mandracchia B, Gennari O, Bramanti A, Grilli S, Ferraro P. Label-free quantification of the effects of lithium niobate polarization on cell adhesion via holographic microscopy. *J Biophotonics*. 2018;11(8):e201700332. doi:10.1002/jbio.201700393
26. Marchesano V, Gennari O, Mecozzi L, Grilli S, Ferraro P. Effects of lithium niobate polarization on cell adhesion and morphology. *ACS Appl Mater Interfaces*. 2015;7(32):18113–18119. doi:10.1021/acsami.5b05340
27. Li J, Mou X, Qiu J, et al. Surface charge regulation of osteogenic differentiation of mesenchymal stem cell on polarized ferroelectric crystal substrate. *Adv Healthc Mater*. 2015;4(7):998–1003. doi:10.1002/adhm.201500032
28. Li YP, Dai XH, Bai YY, et al. Electroactive $BaTiO_3$ nanoparticle-functionalized fibrous scaffolds enhance osteogenic differentiation of mesenchymal stem cells. *Int J Nanomedicine*. 2017;12:4007–4018. doi:10.2147/IJN.S135605
29. Zhang XH, Zhang CG, Lin YH, et al. Nanocomposite membranes enhance bone regeneration through restoring physiological electric microenvironment. *ACS Nano*. 2016;10(8):7279–7286. doi:10.1021/acsnano.6b02247
30. Zhang XH, Cai Q, Liu HY, et al. Osteoconductive effectiveness of bone graft derived from antler cancellous bone: an experimental study in the rabbit mandible defect model. *Int J Oral Maxillofac Surg*. 2012;41(11):1330–1337. doi:10.1016/j.ijom.2012.05.014

31. Zhang WW, Wang J, Gao P, Tan SB, Zhu WW, Zhang ZC. Synthesis of poly(vinylidene fluoride-trifluoroethylene) via a controlled silyl radical reduction of poly(vinylidene fluoride-chlorotrifluoroethylene). *J Mater Chem C*. 2017;5:6433–6441. doi:10.1039/C7TC01051F
32. Zhang CG, Liu WW, Cao C, et al. Modulating surface potential by controlling the beta phase content in poly(vinylidene fluoridetrifluoroethylene) membranes enhances bone regeneration. *Adv Healthc Mater*. 2018;7(11):e1701466. doi:10.1002/adhm.201701466
33. Yao ZH, Song Z, Hao H, et al. Homogeneous/inhomogeneous-structured dielectrics and their energy-storage performances. *Adv Mater*. 2017;29(1601727):1–15. doi:10.1002/adma.201601727
34. Li JJ, Seok S, Chu BJ, Dogan F, Zhang QM, Wang Q. Nanocomposites of ferroelectric polymers with TiO_2 nanoparticles exhibiting significantly enhanced electrical energy density. *Adv Mater*. 2009;21:217–221. doi:10.1002/adma.v21:2
35. Halperin C, Mutchnik S, Agronin A, et al. Piezoelectric effect in human bones studied in nanometer scale. *Nano Lett*. 2004;4(5):1253–1256. doi:10.1021/nl049453i
36. Zhang X, Shen Y, Zhang QH, et al. Ultrahigh energy density of polymer nanocomposites containing $BaTiO_3$@TiO_2 nanofibers by atomic-scale interface engineering. *Adv Mater*. 2015;27:819–824. doi:10.1002/adma.201404101
37. Zhang X, Chen WW, Wang JJ, et al. Hierarchical interfaces induce high dielectric permittivity in nanocomposites containing TiO_2 @$BaTiO_3$ nanofibers. *Nanoscale*. 2014;6:6701–6709. doi:10.1039/c4nr00703d
38. Beloti MM, de Oliveira PT, Gimenes R, Zaghete MA, Bertolini MJ, Rosa AL. In vitro biocompatibility of a novel membrane of the composite poly(vinylidene-trifluoroethylene)/barium titanate. *J Biomed Mater Res A*. 2006;79(2):282–288. doi:10.1002/jbm.a.30801
39. Teixeira LN, Crippa GE, Gimenes R, et al. Response of human alveolar bone-derived cells to a novel poly(vinylidene fluoride-trifluoroethylene)/barium titanate membrane. *J Mater Sci Mater Med*. 2011;22(1):151–158. doi:10.1007/s10856-010-4189-z
40. Vaněk P, Kolská Z, Luxbacher T, et al. Electrical activity of ferroelectric biomaterials and its effects on the adhesion, growth and enzymatic activity of human osteoblast-like cells. *J Phys D: Appl Phys*. 2016;49:175403. doi:10.1088/0022-3727/49/17/175403
41. Zhao M, Bai H, Wang E, Forrester JV, McCaig CD. Electrical stimulation directly induces pre-angiogenic responses in vascular endothelial cells by signaling through VEGF receptors. *J Cell Sci*. 2004;117(Pt 3):397–405. doi:10.1242/jcs.00868
42. Jeong GJ, Oh JY, Kim YJ, et al. Therapeutic angiogenesis via solar cell-facilitated electrical stimulation. *ACS Appl Mater Interfaces*. 2017;9(44):38344–38355. doi:10.1021/acsami.7b13322
43. Ye L, Guan L, Fan P, et al. Effect of a small physiological electric field on angiogenic activity in first-trimester extravillous trophoblast cells. *Reprod Sci*. Aug. 2018;1933719118792102.
44. Chen Y, Ye L, Guan L, et al. Physiological electric field works via the VEGF receptor to stimulate neovessel formation of vascular endothelial cells in a 3D environment. *Biol Open*. 2018;7(9):bio035204. doi:10.1242/bio.035204
45. Augustine R, Dan P, Sosnik A, et al. Electrospun poly(vinylidene fluoride-trifluoroethylene)/zinc oxide nanocomposite tissue engineering scaffolds with enhanced cell adhesion and blood vessel formation. *Nano Res*. 2017;10(10):3358–3376. doi:10.1007/s12274-017-1549-8